Biochem. J. (1990) 272, 743–747 (Printed in Great Britain)

Involvement of an NAD(P)H oxidase as a pO_2 sensor protein in the rat carotid body

Andrew R. CROSS,* Lydia HENDERSON,* Owen T. G. JONES,* Marco A. DELPIANO,† Joachim HENTSCHEL† and Helmut ACKER†‡

*Department of Biochemistry, School of Medical Sciences, University of Bristol, Bristol BS8 1TD, U.K., and †Max-Planck-Institut für Systemphysiologie, Rheinlanddamm 201, D-4600 Dortmund 1, Federal Republic of Germany

The rat carotid body tissue reveals a photometrically measurable haem signal with absorbance maxima at 560 nm, 518 nm and 425 nm, suggesting the presence of a *b*-type cytochrome; this was confirmed by pyridine haemochrome and CO spectra. The quantity of cytochrome *b* was estimated to be 310 pmol·mg of protein^{-1}. This haem is capable of H_2O_2 formation, which can be inhibited by 10 μM-diphenyliodonium (DPI). The hypoxia-induced increase in nervous chemoreceptor discharge and the reduction of FAD and NAD(P)$^+$ were also inhibited by DPI (10 μM). These results suggest that an oxidase such as the NAD(P)H oxidase of neutrophils may act as a pO_2 sensor protein in the rat carotid body, probably inducing the pO_2 chemoreceptor process by H_2O_2 formation.

INTRODUCTION

The carotid body located at the carotid sinus is able to transduce changes of oxygen pressure in the arterial blood into nervous signals regulating respiration and circulation in order to avoid hypoxic situations in the body. The mechanism of the transducing process is still a matter for discussion. A generally accepted concept defines this process as a pO_2-dependent transmitter release from carotid body type I cells, which generates action potentials in post-synaptic nerve endings of the sinus nerve (for review see Acker, 1989). Recent voltage clamp studies have shown that outward K^+ currents of type I cells are inhibited by hypoxia (Hescheler *et al.*, 1989; Lopez-Lopez *et al.*, 1989), and this was substantiated by the observation that the probability of K^+ channels in these cells being open decreased under hypoxia (Delpiano & Hescheler, 1989). Na^+ and Ca^{2+} currents in these cells are unaffected by hypoxia (Hescheler *et al.*, 1989; Lopez-Lopez *et al.*, 1989). The pO_2-dependence of the K^+ channel explains the depolarization of type I cells under hypoxia (Lopez-Lopez *et al.*, 1989), which might lead, by opening of voltage-dependent Ca^{2+} channels, to an influx of Ca^{2+} into the cytosol of these cells. The resulting increased intracellular Ca^{2+} level would facilitate transmitter release via the participation of intracellular Ca^{2+} stores (Pietruschka, 1985; Biscoe *et al.*, 1989; Delpiano & Acker, 1989; Shaw *et al.*, 1989). The molecular mechanism of the inhibitory effect of low pO_2 on K^+ channel activity and thus on the chemoreceptor properties of type I cells is unknown, but the involvement of a haem-type pO_2 sensor protein has been discussed (for a review see Acker, 1989). In a recent publication, Acker *et al.* (1989) described hypoxic light absorbance difference spectra in the rat carotid body which could be inhibited by diphenyliodonium (DPI) (Gatley & Sherratt 1976), a specific inhibitor of the NADPH oxidase in neutrophils (Cross & Jones, 1986). It has been suggested, therefore, that a similar oxidase may be located in the carotid body tissue. The present paper gives a more detailed characterization of an NAD(P)H oxidase in the rat carotid body and considers its possible involvement as a haem-type pO_2 sensor protein in the chemoreceptor process of the carotid body.

MATERIALS AND METHODS

Carotid body preparation and superfusion

After prolonged flushing of the common carotid arteries with Macrodex 6% (Knoll, Glandorf, Germany) to eliminate red blood cells from the tissue, carotid bodies with the intact sinus nerve and the immediate vessels were excised from rats anaesthetized with pentobarbitone (3–4 mg/rat) and heparinized with 1300 units/rat. The carotid bodies were denuded of all other structures, and either sampled for spectral analysis or placed in a small Lucite chamber mounted on the stage of an upright microscope (Olympus, Hamburg, Germany) for FAD and NADPH fluorescence measurements and nervous chemoreceptor discharge recordings. The cleaned organs (length 500 μm, width 300 μm, thickness 150 μm) were then superfused with modified Locke's solution, as described by Delpiano & Acker (1989), equilibrated with different O_2 mixtures with the aid of a gas mixing pump (Wösthoff, Bochum, Germany) and viewed with a 40 × water immersion objective lens and 10 × ocular lenses. Oxygenation of the superfusion medium was monitored close to the tissue with a needle pO_2 electrode whose tip was located near the objective lens. Temperature was routinely maintained at about 35 °C and pH was kept at 7.36.

Spectral analysis

Carotid bodies ($n = 35$) were suspended in 1 ml of phosphate-buffered saline, pH 7.2, and sonicated for three cycles of 20 s at 50 W with a Branson Soniprobe, with 30 s of cooling in an ice/water bath between each cycle. Reduced minus oxidized difference spectra were recorded on a sensitive split-beam spectrophotometer as described by Cross *et al.* (1984). Briefly, sonicated samples were split into two 400 μl aliquots and a baseline was recorded eight times and averaged; a few grains of solid sodium dithionite were added to the sample cuvette and the spectrum was re-recorded and averaged. The baseline spectrum was then subtracted from the reduced spectrum. CO difference spectra were obtained by bubbling a stream of CO through the sample for 30 s before recording the spectrum. Pyridine haemo-

Abbreviation used: DPI, diphenyliodonium.

‡ To whom correspondence and reprint requests should be addressed.

chrome spectra were obtained by treatment of samples with alkaline pyridine before recording difference spectra (Smith, 1975).

Measurement of H_2O_2 production

Dihydrorhodamine 123 and rhodamine 123 (Molecular Probes, Eugene, OR, U.S.A.) were dissolved in dimethyl sulphoxide to give stock solutions of 50 mM. The dihydrorhodamine was stored under N_2. The non-fluorescent dihydrorhodamine is converted to rhodamine in the reaction with H_2O_2 (Rothe *et al.*, 1988). This fluorescent positively charged dye is taken up by cells. The conversion of dihydrorhodamine 123 to rhodamine 123 by a superoxide-generating system is insensitive to superoxide dismutase but sensitive to catalase. This indicates that H_2O_2, but not $O_2^{\cdot-}$ itself, reacts with dihydrorhodamine.

Images of the fluorescent cells were obtained using a Bio-Rad MRC-500 confocal scanning optical microscope mounted on a Nikon inverted microscope. The bath solution was maintained at 37 °C by an infra-red lamp linked to a thermocouple. The carotid body was placed over a 50× objective lens in a buffered physiological saline solution containing 67 μM-dihydrorhodamine, and the images were recorded several minutes later.

NAD(P)H and FAD fluorescence photometry

Light from a xenon arc-lamp (ILC Technology, Sunnyvale, CA, U.S.A.), which was filtered for NAD(P)H fluorescence excitation by a 366 nm interference filter (Schott) and for FAD fluorescence excitation by a 460 nm interference filter (Schott), both with a half-bandwidth of 7 nm, transilluminated the carotid body tissue. The spectrum of the emitted light from the tissue passed through a cut-off filter [400 nm for NAD(P)H fluorescence and 490 nm for FAD fluorescence). Spectra were analysed using a Veril-S-60 filter (Leitz, Wetzlar, Germany) and recorded with a photomultiplier (EMI 9502A; Hayes, Middx., U.K.), both placed on the third ocular tube of the microscope trinocular head. NAD(P)H fluorescence was measured at 459 ± 2 nm ($n = 6$) and FAD fluorescence at 535 ± 4 nm ($n = 6$).

Light microscopy

The excised carotid body was fixed by immersion for 1 h in 0.025 M-sodium cacodylate-buffered 2% glutaraldehyde (20 °C, pH 7.4), washed with the same buffer and post-fixed for 2 h in 2% OsO_4 (4 °C, pH 7.4). After dehydration in increasing concentrations of ethanol (up to 70%) the tissue was contrasted with 1% uranyl acetate plus 1% phosphotungstic acid in 70% ethanol overnight (4 °C), followed by complete dehydration. The sample was embedded, via the intermediary medium propylene oxide, in Epon 812. Semi-thin sectioning (1 μm) was carried out on a Reichert Ultracut E. Sections stained with Richardson Toluidene Blue solution were viewed and photographed with a Leitz Dialux 20 light microscope.

Materials

DPI was synthesized as described by Collette *et al.* (1956).

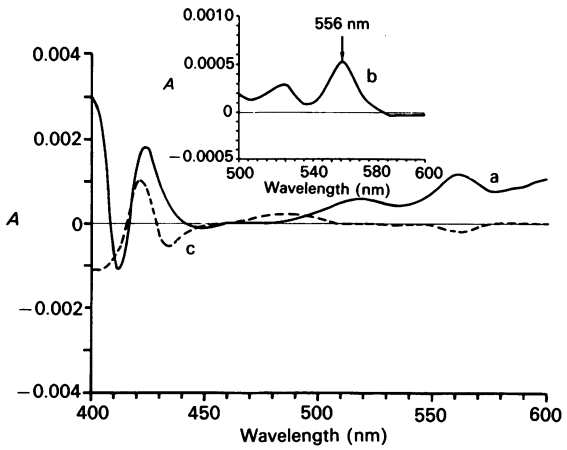

Fig. 1. Absorbance spectra of carotid body preparations

Samples were prepared and absorbance spectra were determined as described in the Materials and methods section. Trace a, dithionite-reduced minus air-oxidized difference spectrum of sonicated carotid bodies; b, reduced minus oxidized pyridine haemochrome spectrum; c, spectrum of the dithionite-reduced preparation after CO treatment minus the dithionite-reduced spectrum.

Afferent chemoreceptor discharge recording

Chemoreceptor discharge was recorded from the sinus nerve by the method of Delpiano & Acker (1989). Briefly, multifibre filaments (5–20 active fibres) lifted into a paraffin oil pool above the superfusion medium were recorded with the aid of a unipolar platinum electrode and displayed on a dual-beam storage oscilloscope (Textronik 5113; Köln, Germany). The amplified spikes were fed into a window discriminator, counted with a ratemeter and audiomonitored. NAD(P)H and FAD fluorescence, as well as the chemoreceptor discharge rate, were monitored with a multipen ink recorder (Rikadenki, Freiburg, Germany).

RESULTS AND DISCUSSION

Reduced minus oxidized difference spectra revealed the presence of a haem signal with absorbance maxima at 560 nm, 518 nm and 425 nm, suggesting a *b*-type cytochrome (Fig. 1, spectrum a). The presence of protohaem as the prosthetic group was confirmed by the pyridine haemochrome spectrum, which had the characteristic absorbance maximum of the band centred at 556–557 nm (Porra & Jones, 1963) (Fig. 1, spectrum b). Using a molar absorption coefficient of 21.6 $mM^{-1} \cdot cm^{-1}$, the quantity of cytochrome *b* was estimated to be 310 pmol·mg of $protein^{-1}$. Neither NADH (1 mM) nor NADPH (1 mM) caused detectable reduction of the cytochrome. The lack of reduction by these electron donors may be due to disruption of the system during sonication, rapid re-oxidation of reduced haem by molecular oxygen or the requirement for another electron donor. Haem

Fig. 2. Light microscopic and rhodamine 123 confocal images of a carotid body

The carotid body was prepared for light microscopy (left side) and incubated with dihydrorhodamine 123, and images (right side) were obtained as described in the Materials and methods section. Only the highly fluorescent cells are within the plane of focus of the objective lens. The fluorescence intensity is shown in pseudocolours and increases from blue to red. Bar = 100 μm. cb, carotid body; sn, sinus nerve. A cluster of type I cells is indicated by the circle.

Fig. 3. Rhodamine 123 confocal images of carotid body cells

Higher magnification images of an area of the carotid body tissue. Bar = 50μm.

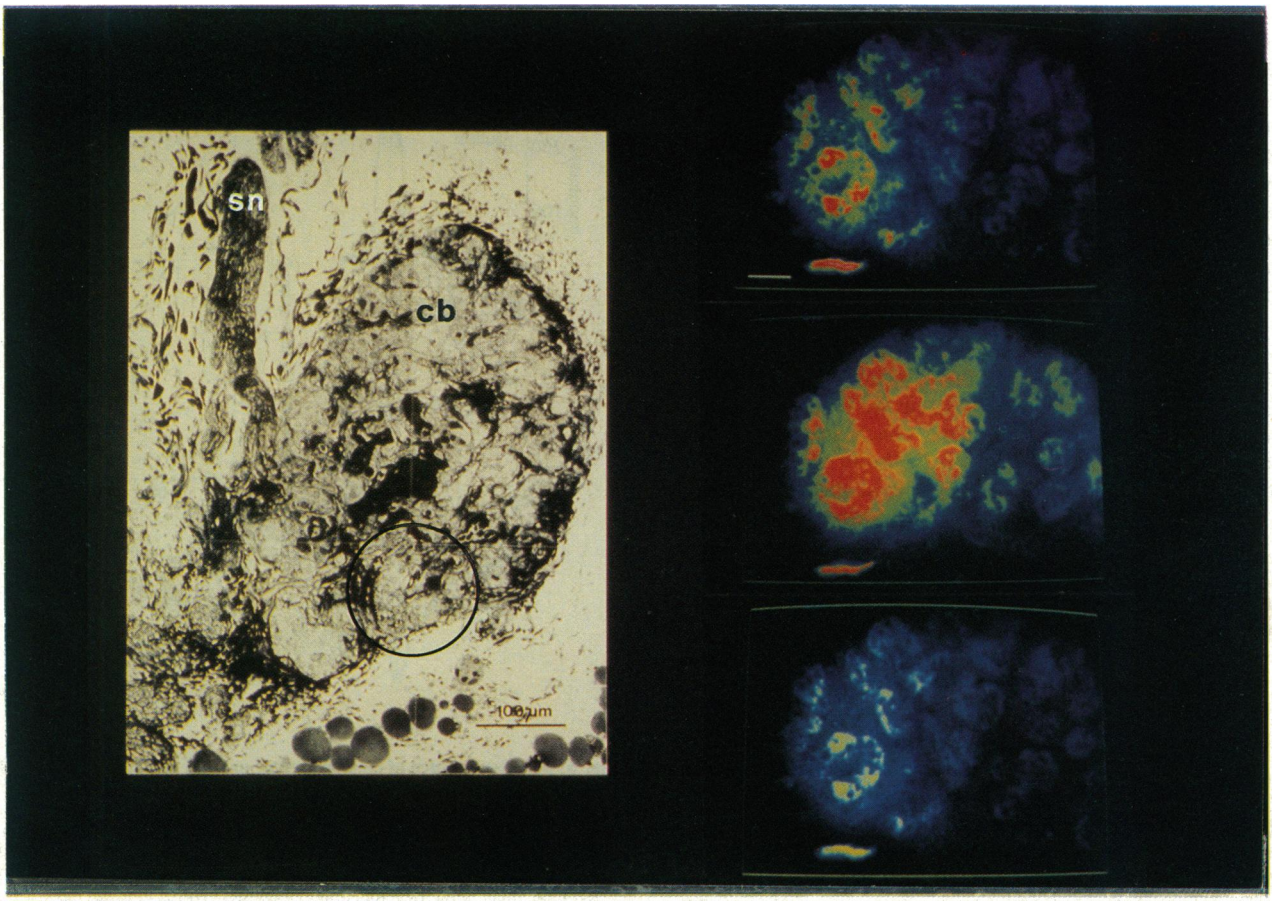

Fig. 2. For caption see facing page.

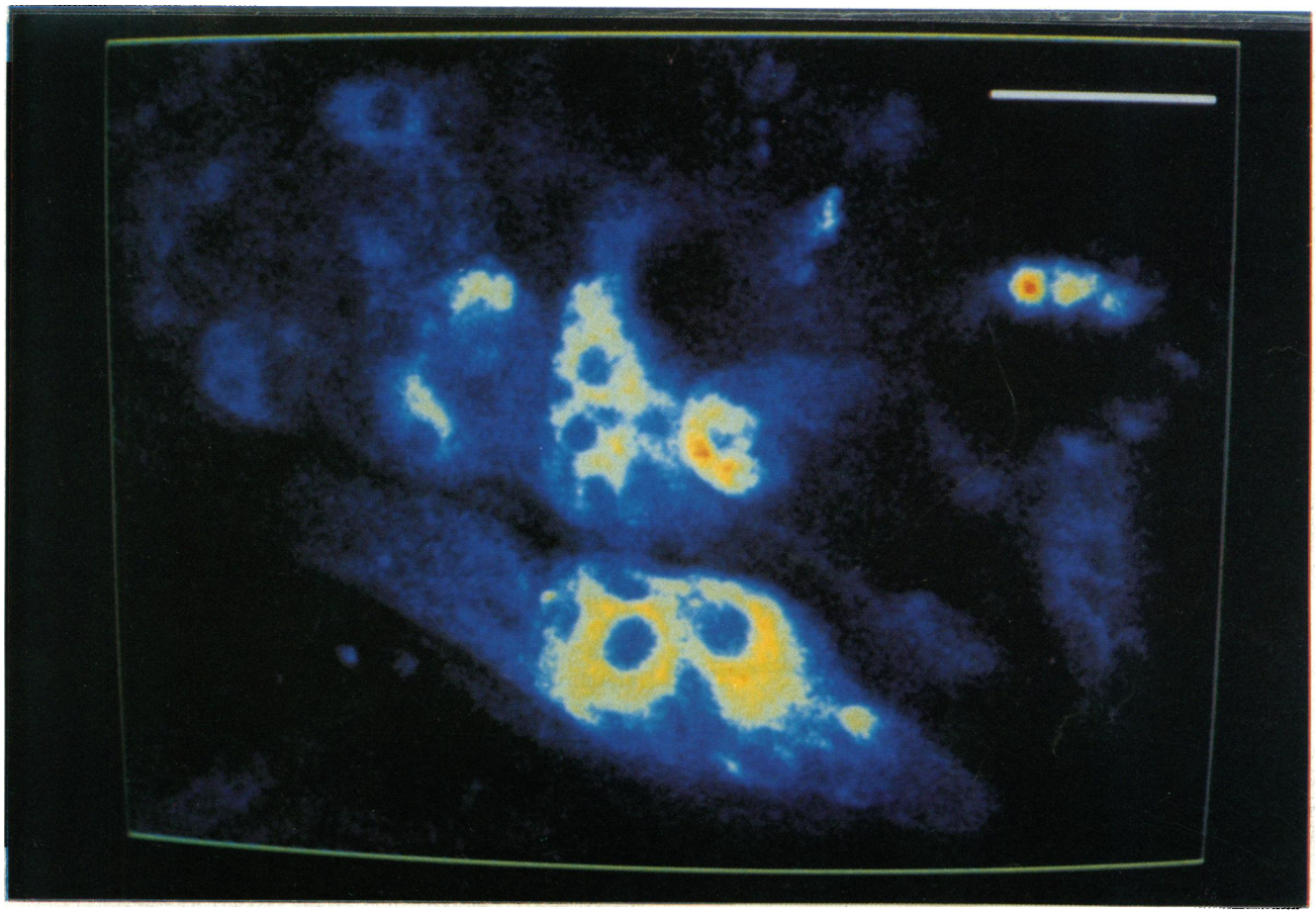

Fig. 3. For caption see facing page.

proteins that react with oxygen frequently bind CO. The dithionite-reduced carotid body preparation formed a complex with CO (Fig. 1, spectrum c) with troughs around 560 and 430 nm and a peak at 420 nm. It is apparent from the size of the spectral changes that not all of the haem is complexed to CO, and in this respect the CO-binding characteristics are similar to those of the neutrophil cytochrome b_{-245} (Cross *et al.*, 1981, 1982), which is believed to be the terminal oxidase in the NADPH-dependent superoxide-generating system of phagocytic cells. Cytochrome b_{-245} also has a low affinity for CO (K_m = 1.4 mM) (Cross *et al.*, 1982), despite a much higher affinity for O_2 (K_m = 5–30 μM) (Gabig *et al.*, 1979; Gabig & Babior, 1979; Kakinuma & Kaneda, 1982; Edwards *et al.*, 1983; Morel *et al.*, 1985). The low CO affinity of the carotid body haem we describe here is in accordance with other measurements, which showed that the chemoreceptor discharge of the carotid body also has a low affinity for CO and first starts to increase in acute experiments at 63% saturation of haemoglobin by CO (Lahiri, 1980).

H_2O_2 production

The confocal microscope scans and collects emitted light from only within the plane of focus of the objective lens (Shotton & White, 1989). Therefore the image obtained is the fluorescence from a discrete slice within the whole tissue. Non-fluorescent cells are not visible.

Fig. 2 (left) shows a light microscopic picture of a cross-section through a carotid body. The typical carotid body tissue (cb) with clusters of type I cells and sinus nerve (sn) are to be seen. As an example, one cluster of type I cells is marked by a circle. These typical clusters are also visible on the right side, where three optical cross-sections at different depths through a carotid body, which has been incubated in dihydrorhodamine, are shown. The highly fluorescent cells are in the plane of the focus (red colours).

Fig. 3 shows an area of the carotid body under higher magnification (bar 50μm). The fluorescent cytosol round the nucleus is clearly visible. The generation of rhodamine 123 (shown by fluorescence) suggests that the tissue is producing H_2O_2. Images were obtained from carotid bodies maintained at room temperature for periods of greater than 20 min before the addition of dihydrorhodamine 123. However, no image was obtained from a carotid body which had been incubated at room temperature in 10 μM-DPI for 20 min. This suggests that the generation of rhodamine was due to a specific DPI-inhibitable activity of the tissue. The DPI-treated carotid body was washed and incubated in 67 μM-rhodamine. After washing to remove the excess external dye, images of the tissue were obtained. These indicated that, in the DPI-treated tissue, the cells still maintained a membrane potential, and so were living. These results suggest that the carotid body is capable of generating H_2O_2 in a DPI-inhibitable way.

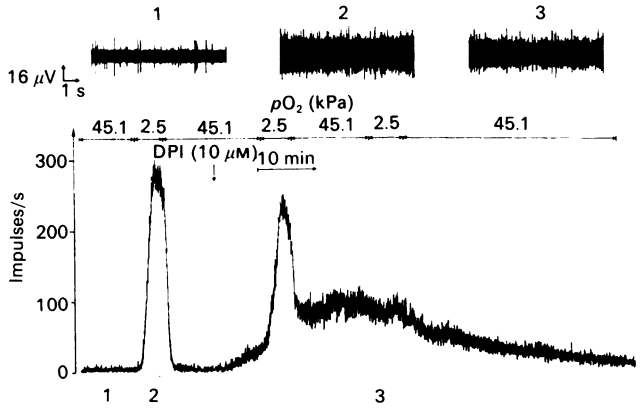

Fig. 4. Nervous chemoreceptor response to hypoxia and DPI

Nervous chemoreceptor discharge was recorded from the sinus nerve as described in the Materials and methods section. The Figure shows original recordings of the sinus nerve action potentials photographed at points 1, 2 and 3 during the experiment; pO_2 level in the superfusion medium and integrated nervous chemoreceptor activity are shown.

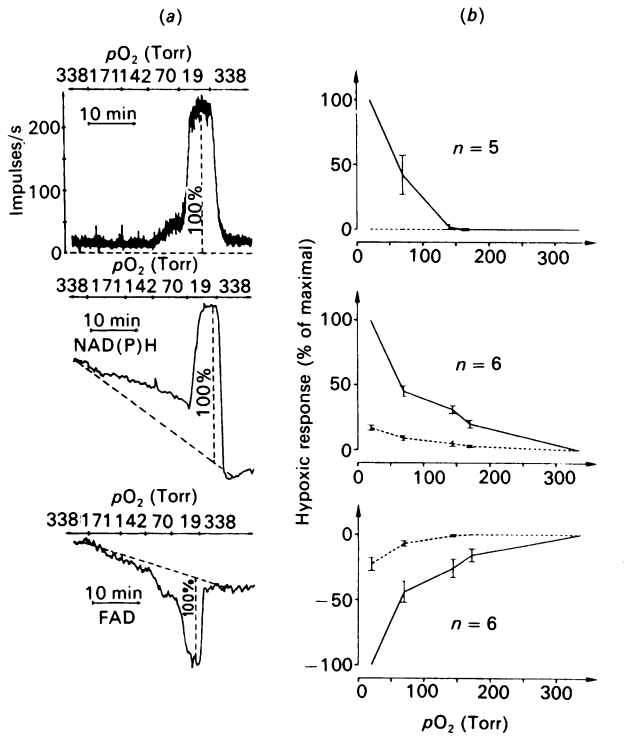

Fig. 5. pO_2-dependence of chemoreceptor activity and NAD(P)H and FAD fluorescence

(*a*) Nervous chemoreceptor discharge and NAD(P)H and FAD fluorescence changes during stepwise changes of the pO_2 in the superfusion medium are given from three different experiments. The broken lines give the baselines and the 100% values. Response curves of the three measured parameters to pO_2 are shown. Values are means ± S.E.M. The broken lines are response curves in the presence of DPI (10 μM). 1 Torr = 133.3 Pa.

Relationship between chemoreceptor discharge and NAD(P)H/FAD fluorescence

Fig. 4 shows the effects of hypoxia and DPI on the chemoreceptor nervous discharge of the carotid body. Lowering the pO_2 in the superfusion medium from 45.1 kPa to 2.5 kPa resulted in a typical increase in chemoreceptor discharge (Delpiano & Acker, 1989). Addition of DPI (10 μM) to the superfusion medium induced an increase in the basal nervous activity, which slowly declined and reached control values after about 1 h. A second hypoxic stimulation 10 min after DPI application again resulted in an increase in chemoreceptor activity, but a third one, after about 27 min, did not induce a response. This irreversible inhibition of the hypoxia-induced nervous chemoreceptor response at about 27 min after DPI application was observed in ten experiments. The result indicates that DPI is not impairing action potential generation in the post-synaptic nerve endings of the sinus nerve, but that DPI must act specifically on the pO_2-dependent chemoreceptor process in the carotid body.

The pO_2 in the medium was changed stepwise from 45.1 kPa to 2.5 kPa, and this change was correlated with the nervous chemoreceptor activity (n = 5), the NAD(P)H fluorescence (n =

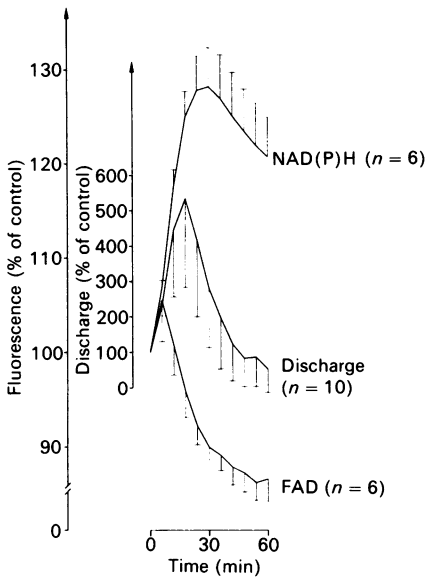

Fig. 6. Change in chemoreceptor discharge as well as in NAD(P)H and FAD fluorescence in the presence of DPI (10 μM)

Values are given as percentages of control; i.e. normoxic conditions without DPI. Reduction of $NAD(P)^+$ and FAD are clearly to be seen, as is the initial excitation of the chemoreceptor discharge.

6) and the FAD fluorescence ($n = 6$), as shown in Fig. 5. Fig. 5(*a*) gives examples for the three parameters from three different experiments. By relating, in each experiment, the changes at the different pO_2 values to the maximal response (100 %), the mean response curves of the three parameters were obtained (Fig. 5*b*) under control conditions (solid lines) and in the presence of DPI (broken lines). The pO_2 at the half-maximal value of the response curve under control conditions was 8.4 kPa for the chemoreceptor discharge, 8.8 kPa for the NAD(P)H fluorescence and 8.7 kPa for the FAD fluorescence. This similarity of the half-maximal values hints at a close interaction between the three parameters during the chemoreceptive process in the carotid body under hypoxia. DPI application led to a complete inhibition of the hypoxia-induced nervous chemoreceptor response and to an attenuation of the fluorescence changes.

Fig. 6 shows the mean time course of the response of chemoreceptor discharge ($n = 10$) and NAD(P)H ($n = 6$) and FAD ($n = 6$) fluorescence to DPI application. The control value of the different parameters before administering DPI was taken as 100 % for this purpose. It can be seen that $NAD(P)^+$ and FAD become reduced, as during hypoxia, whereas the chemoreceptor activity, after an initial increase, declined to values slightly below control. A stabilization of the values was reached after 1 h. The time course of the chemoreceptor discharge is similar to that of nerve recordings under prolonged hypoxia in the carotid body *in vitro* (Delpiano & Acker, 1989), where a decline of the chemoreceptor discharge after an initial increase can also be observed (Delpiano & Acker, 1989).

It might therefore be speculated that the presumed interaction of DPI with the haem protein mimics, at least partly, the pO_2 chemoreception in the carotid body by preventing electron transfer through the oxidase and consequently H_2O_2 formation. However, future experiments will have to give stronger support for this speculative pO_2-dependent H_2O_2 formation and its possible importance for pO_2 chemoreception in the carotid body. The following two hypotheses are attractive to study in this context. The involvement of H_2O_2 in pO_2 chemoreception was proposed by Sies (1977), with the model that glutathione peroxidase degrades hydroperoxides and thereby induces a transition in the GSH/GSSG redox system, which as the major cellular pool of mobile thiol groups can change protein formations, e.g. for ion channels. Another possibility for the regulation of ion channel conductivity is that the haem protein in the carotid body is linked to guanylate cyclase, as described in the bovine lung (Gerzer *et al.*, 1981), thus regulating the cyclic GMP content, which is known to decrease in the carotid body under hypoxia (Wary *et al.*, 1989).

Received 2 July 1990/22 August 1990; accepted 3 September 1990

REFERENCES

Acker, H. (1989) Annu. Rev. Physiol. **51**, 835–844
Acker, H., Dufau, E., Huber, J. & Sylvester, D. (1989) FEBS Lett. **256**, 75–78
Biscoe, T. J., Duchen, M. R., Eisner, D. A., O'Neill, S. C. & Valdeomillos, M. (1989) J. Physiol. (London) **416**, 421–434
Collette, J., McGreer, D. & Crawford, R. (1956) J. Am. Chem. Soc. **78**, 3819–3820
Cross, A. R. & Jones, O. T. G. (1986) Biochem. J. **237**, 111–116
Cross, A. R., Jones, O. T. G., Harger, A. M. & Segal, A. W. (1981) Biochem. J. **194**, 599–606
Cross, A. R., Higson, F. K., Jones, O. T. G., Harger, A. M. & Segal, A. W. (1982) Biochem. J. **204**, 479–485
Cross, A. R., Parkinson, J. F. & Jones, O. T. G. (1984) Biochem. J. **223**, 337–343
Delpiano, M. A. & Acker, H. (1989) Brain Res. **482**, 235–246
Delpiano, M. A. & Hescheler, J. (1989) FEBS Lett. **249**, 195–198
Edwards, S. W., Hallett, M. B., Lloyd, D. & Campbell, A. K. (1983) FEBS Lett. **161**, 60–64
Gabig, T. G. & Babior, B. M. (1979) J. Biol. Chem. **254**, 9070–9074
Gabig, T. G., Bearman, S. J. & Babior, B. M. (1979) Blood **53**, 1133–1139
Gatley, J. S. & Sherratt, H. S. A. (1976) Biochem. J. **158**, 307–315
Gerzer, R., Böhme, E., Hofmann, F. & Schultz, G. (1981) FEBS Lett. **132**, 71–74
Hescheler, J., Delpiano, M. A., Acker, H. & Pietruschka, F. (1989) Brain Res. **486**, 79–88
Kakinuma, K. & Kaneda, M. (1982) Adv. Exp. Med. Biol. **141**, 351–360
Lahiri, S. (1980) Fed. Proc. Fed. Am. Soc. Exp. Biol. **39**, 2648–2652
Lopez-Lopez, J., Gonzales, C., Urena, J. & Lopez-Barneo, J. (1989) J. Gen. Physiol. **93**, 1001–1015
Morel, F., Doussiere, J., Stasia, M.-J. & Vignais, P. V. (1985) Eur. J. Biochem. **152**, 699–679
Pietruschka, F. (1985) Brain Res. **347**, 140–143
Porra, R. J. & Jones, O. T. G. (1963) Biochem. J. **87**, 186–192
Rothe, G., Oser, A. & Valet, G. (1988) Naturwissenschaften **75**, 354–355
Shaw, K., Montague, W. & Pallot, D. J. (1989) Biochim. Biophys. Acta **1013**, 42–46
Shotton, D. & White, N. (1989) Trends Biochem. Sci. **14**, 435–439
Sies, H. (1977) in Tissue Hypoxia and Ischemia (Ruvich, M., Coburn, R., Lahiri, S. & Clance, B., eds.), pp. 51–66, Plenum Publishing Corp., New York
Smith, K. M. (1975) in Porphyrins and Metalloporphyrins (Smith, U. M., ed.), pp. 804–807, Elsevier, Amsterdam and New York
Wary, W. J., Cheng, G. F., Dinger, B. G. & Fidone, S. J. (1989) Neurosci. Lett. **105**, 164–168